Breaking of Valley Degeneracy by Magnetic Field in Monolayer MoSe_{2}

David MacNeill, Colin Heikes, Kin Fai Mak, Zachary Anderson, Andor Kormányos, Viktor Zólyomi, Jiwoong Park, and Daniel C. Ralph

Breaking of valley degeneracy by magnetic field in monolayer MoSe$_2$

David MacNeill, Colin Heikes, and Zachary Anderson

Department of Physics, Cornell University, Ithaca, NY 14853, USA

Kin Fai Mak and Daniel C. Ralph

Department of Physics, Cornell University, Ithaca, NY 14853, USA and

Kavli Institute at Cornell, Cornell University, Ithaca, NY 14853, USA

Andor Kormányos

Department of Physics, University of Konstanz, D-78464 Konstanz, Germany

Viktor Zólyomi

Department of Physics, Lancaster University,

Lancaster LA1 4YB, United Kingdom

Jiwoong Park

Department of Chemistry and Chemical Biology,

Cornell University, Ithaca, NY 14853, USA and

Kavli Institute at Cornell, Cornell University, Ithaca, NY 14853, USA

(Dated: December 22, 2014)

Abstract

Using polarization-resolved photoluminescence spectroscopy, we investigate breaking of valley degeneracy by out-of-plane magnetic field in back-gated monolayer MoSe$_2$ devices. We observe a linear splitting of $-0.22 \frac{\text{meV}}{\text{T}}$ between luminescence peak energies in σ_+ and σ_- emission for both neutral and charged excitons. The optical selection rules of monolayer MoSe$_2$ couple photon handedness to the exciton valley degree of freedom, so this splitting demonstrates valley degeneracy breaking. In addition, we find that the luminescence handedness can be controlled with magnetic field, to a degree that depends on the back-gate voltage. An applied magnetic field therefore provides effective strategies for control over the valley degree of freedom.

Monolayer MoSe$_2$ and other monolayer transition metal dichalcogenides (TMDs) are a materials system with unique potential for controlling their valley degree of freedom [1–8]. Similar to graphene, the conduction and valence band show extrema (valleys) at the vertices of a hexagonal Brillouin zone; unlike graphene, MoSe$_2$ exhibits a nonzero optical gap of 1.66 eV [9, 10]. This has allowed exploration of optoelectronic properties arising from the valley-dependent chirality of massive Dirac fermions, predicted in the context of inversion symmetry broken graphene [11, 12]. This chirality leads to optical selection rules coupling the exciton valley degree of freedom to photon handedness [2–7]. Using polarization-resolved spectroscopy researchers have demonstrated valley-selective luminescence with near 100% fidelity [2, 7]. Furthermore, the ability to pump valley-polarized carriers with circularly-polarized light has been demonstrated through the valley Hall effect [8]. The chiral electronic states are also predicted to posses valley-contrasting orbital magnetic moments coupling valley pseudospin to magnetic field [11–17], which opens up the possibility for magnetic control over the valley degree of freedom [13, 18].

Here, we demonstrate the use of magnetic fields to break valley degeneracy in a monolayer TMD. Specifically, we report polarization-resolved luminescence spectra for back-gated MoSe$_2$ devices at 4.2 K and in magnetic fields up to 6.7 T. We study the luminescence peak energies as a function of magnetic field, finding a linear splitting of $-0.22\frac{\text{meV}}{\text{T}}$ between peaks corresponding to light emission with different senses of circular polarization, σ_+ and σ_-. We interpret this as a Zeeman splitting due to valley-dependent magnetic moments. We also investigate the magnetic field dependence of luminescence handedness, finding that the emission becomes circularly-polarized in magnetic field even with unpolarized excitation, and that the degree of this polarization can be increased to about 50% by gating the sample. This suggests that electric fields can facilitate the generation of valley-population imbalance in samples where valley degeneracy has been broken by magnetic field. Our results demonstrate a recently-proposed [18] strategy for generating valley populations, and could lead to new approaches for controlling the valley degree of freedom in monolayer TMDs.

Our device geometry and measurement apparatus are shown in Fig. 1a and 1b. All measurements were taken using a scanning confocal microscope integrated with a 7 T superconducting magnet dewar, with light coupled in and out of the system via a polarization-maintaining optical fiber (similar designs were reported in Refs. [19, 20]). The light is focused into a roughly 1 μm diameter spot using a pair of aspheric lenses, and the sample is scanned
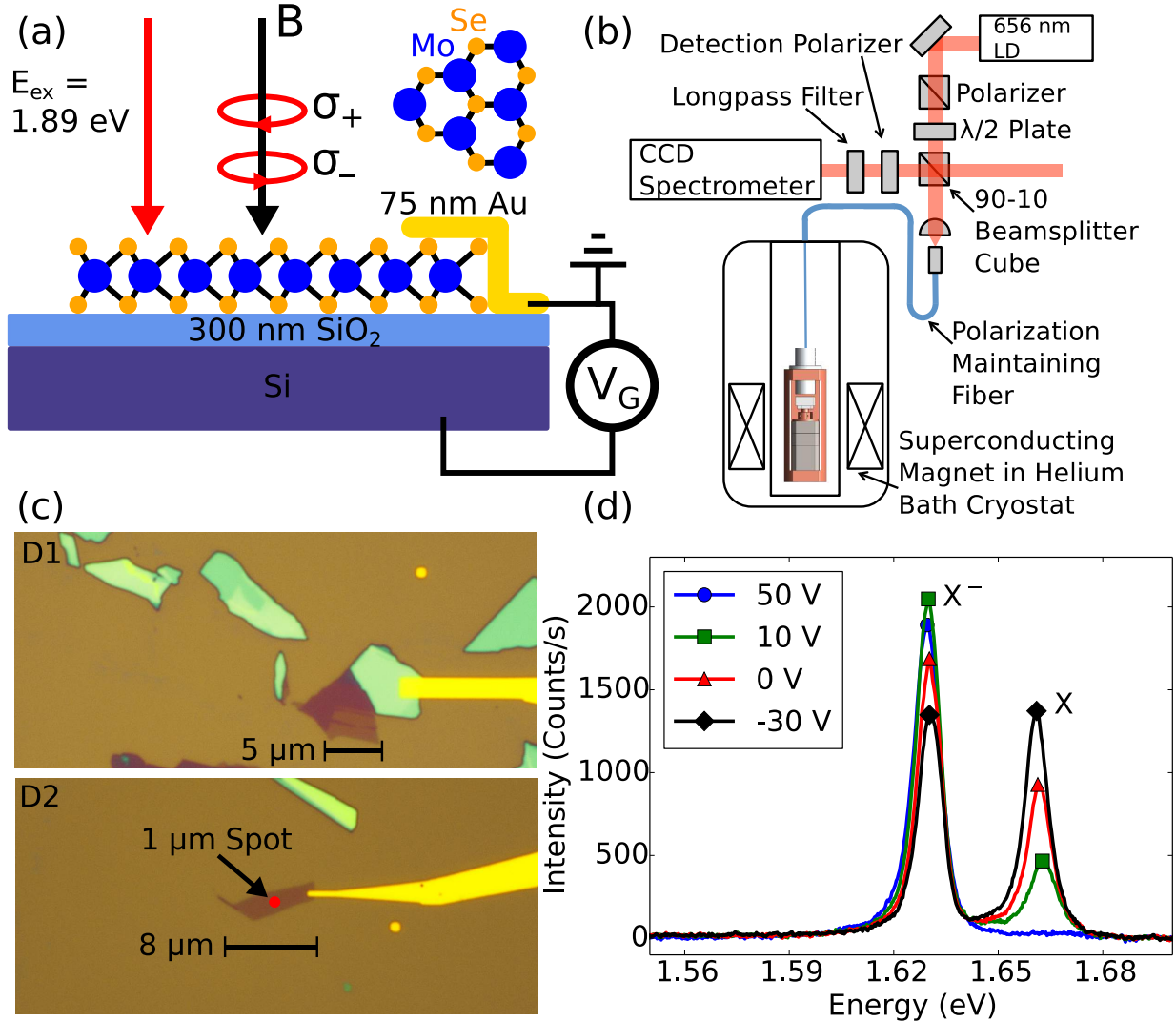
2

FIG. 1. (color online). (a) Experimental geometry showing back-gated monolayer $MoSe_2$ devices in out-of-plane magnetic fields. Luminescence is excited with light from a 1.89 eV laser diode and collected separately for σ_+ and σ_- polarization in the Faraday geometry. (b) Schematic of the fiber-coupled optical cryostat used in the experiment. (c) Optical micrographs of devices D1 and D2. (d) Luminescence spectra of D2 taken at 0 T and 4.2 K with -30 V, 0 V, 10 V, and 50 V back-gate voltage.

using piezo-driven nanopositioners (from attocube). The sample, positioners, and optical components are placed in a vacuum cryostat which is then evacuated and lowered into a helium bath containing a superconducting magnet; helium exchange gas is added to ensure

thermalization of the sample at 4.2 K. For the data in the main text, the excitation power was between 10-60 μW.

To enable polarization-resolved spectroscopy, a zero-order quartz $\lambda/4$ plate is placed between the aspheric lenses, oriented at 45° to the fiber axes; this couples σ_+ and σ_- emission into orthogonal polarization modes of the fiber. The light exiting the fiber is directed though a rotatable polarizer, which selects one fiber mode for spectral analysis by a thermoelectrically cooled CCD spectrometer. We can also create circularly-polarized excitation by coupling linearly-polarized light into one of the two fiber polarization modes, or create equal intensity excitation in σ_+ and σ_- polarization by coupling in light polarized at 45° to the fiber axes. We excite photoluminescence with light from a 1.89 eV laser diode, which is 230 meV blueshifted from the A exciton transition, and as a result we see little dependence of the emission polarization on excitation polarization (see supplement section 1 [21]). The conclusions discussed below are independent of excitation polarization.

To fabricate our samples, we exfoliate bulk MoSe$_2$ crystals (grown by direct vapor transport) onto 300 nm silicon oxide on silicon, then use electron-beam lithography to define a single 0.5 nm Ti/75 nm Au contact, allowing use of the silicon substrate as a back gate. All data shown in the main text were taken from devices D1 and D2 pictured in Fig. 1c. Figure 1d shows the $B = 0$ luminescence spectra of D2 at -30 V, 0 V, 10 V, and 50 V. The peaks at 1.66 eV and 1.63 eV correspond to the neutral and charged A exciton respectively, with a charged exciton (trion) binding energy of 30 meV [9]. As the back-gate voltage is increased the exciton luminescence decreases and the trion luminescence increases, showing that our samples are intrinsically n-type and that the 1.63 eV peak corresponds to negatively charged trion luminescence.

Figure 2a compares polarization-resolved spectra taken for D1 in out-of-plane magnetic fields of 0 T, 6.7 T and -6.7 T and with the back gate grounded. For these data, we excite photoluminescence using equal intensity excitation in σ_+ and σ_- polarization. At zero field, we find no significant dependence of the peak energies or intensities on emission handedness. In comparison, the spectra taken at 6.7 T show splitting between the σ_+ and σ_- emission peaks of about -1.5 meV for both the exciton and trion. The luminescence is also σ_+ polarized: the trion peak has $P_{\text{trion}} = \frac{I_+ - I_-}{I_+ + I_-} = 14\%$, where $I_\pm$ is the peak intensity of the trion in $\sigma_\pm$ detection. For the exciton we measure $P_{\text{exciton}} = 9\%$. The luminescence polarization changes sign with reversal of the magnetic field but not with excitation polarization, showing
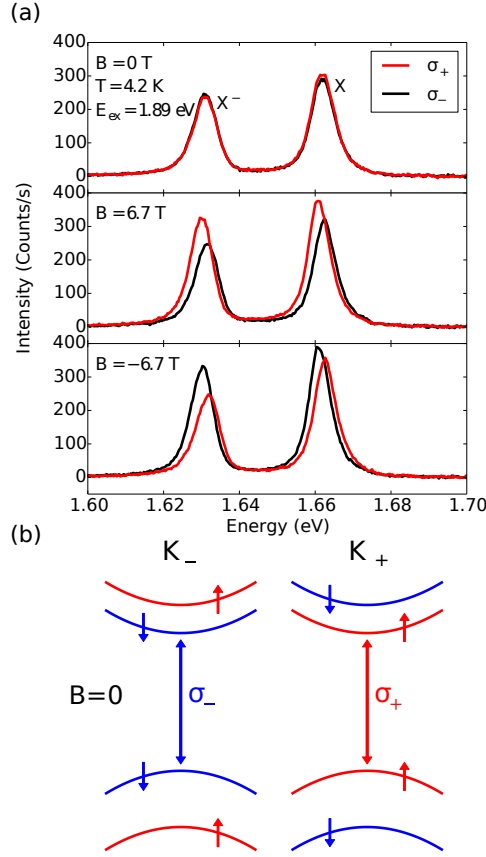
FIG. 2. (color online). (a) Polarization-resolved luminescence spectra from monolayer $MoSe_2$ (D1) at 4.2 K for σ_+ and σ_- detection, as excited using unpolarized light at 1.89 eV. From top to bottom the panels show spectra taken with 0 T, 6.7 T and -6.7 T out-of-plane magnetic field. Both the polarization and splitting change sign upon reversing the field as shown in the lower panel. (b) Schematic bandstructure of $MoSe_2$ near the K_+ and K_- points in zero magnetic field, showing the optical selection rules for the A exciton transition studied in this experiment. Within each valley, spin degeneracy is broken at $B = 0$ due to spin-orbit coupling, [9, 10, 13, 22, 23]. The arrows denote spin angular momentum up and down for the occupied states.

that it arises from magnetically induced changes in the exciton and trion populations. Figure 2b depicts the schematic bandstructure of a $MoSe_2$ monolayer, illustrating the direct band gaps at the K_+ and K_- points, with arrows indicating the allowed A exciton transitions for $\sigma_\pm$ light. Since the emission handedness is coupled to the exciton valley degree of freedom, the peak splitting and polarization we observe indicate valley degeneracy breaking.
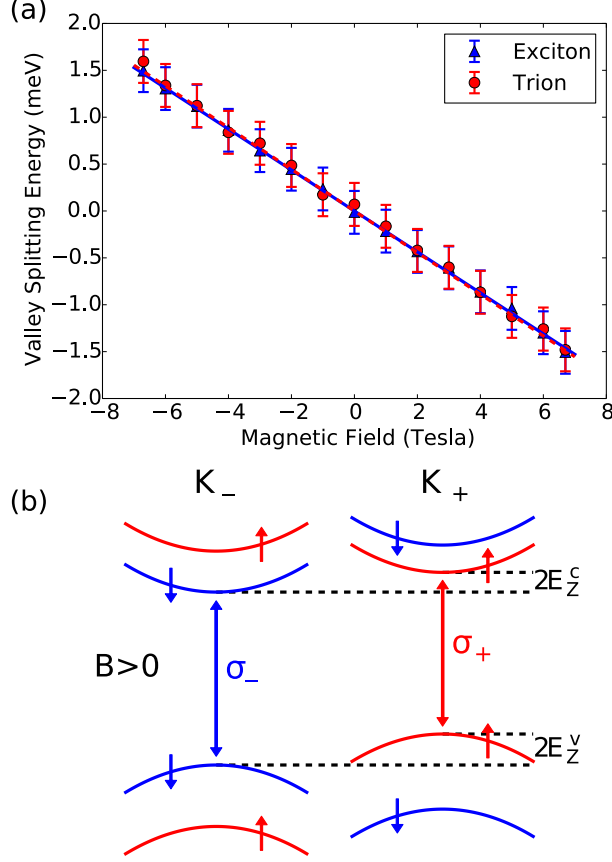
5

FIG. 3. (color online) (a) Difference of peak energies found for σ_+ and σ_- detection plotted versus magnetic field for D1. Both the exciton (blue triangles) and trion (red circles) show splitting of $-0.22 \pm 0.01 \frac{\text{meV}}{\text{T}}$ found via a linear fit. The fits are plotted as blue solid and red dashed lines for the exciton and trion respectively. (b) The schematic bandstructure of MoSe$_2$ in magnetic field showing the Zeeman energy $E_Z^{c(v)}$ for the conduction (valence) band. The exciton Zeeman splitting is $2\left(E_Z^c - E_Z^v\right)$.

Figure 3a shows the valley splitting of the exciton and trion peaks, defined as the difference between peak luminescence energy in σ_+ and σ_- detection, versus magnetic field. For each data point the peak positions were extracted via fits to a phenomenological asymmetric Voigt line shape (see supplement section 2 [21]). The error bars come primarily from the CCD pixel size (about 0.15 nm per pixel). For both the exciton and trion peaks the valley splitting shows a linear magnetic-field dependence with a slope of $-0.22 \pm 0.01 \frac{\text{meV}}{\text{T}}$. Similar results were found on three separate samples; data from other samples are given in supplement

section 3 [21].

Valley splitting in magnetic field arises from the intrinsic chirality of Bloch electrons at the K_+ and K_- points. States at the two valley edges are Kramer's doublets related by time-reversal symmetry, so that their degeneracy can be broken by breaking time-reversal symmetry. Bloch electrons in a given band carry spin and orbital magnetic moments which change sign between valleys [11, 12, 24, 25]. Figure 3b schematically shows the energy shifts arising from Zeeman coupling between these moments and the magnetic field; there we define $2E_Z^{c(v)}$ as the magnetic-field-induced energy difference between the K_+ and K_- valley at the conduction (valence) band edge. Magnetoluminescence spectroscopy probes only the exciton Zeeman energy, which is the difference between conduction and valence band Zeeman energies. In this difference, the contributions from spin magnetic moments are expected to cancel, leaving only the contributions from orbital magnetic moments. The measured sign and magnitude of the valley splitting can be understood within a tight-binding picture [26, 27]. In the K_τ valley (letting $\tau = \pm 1$ be the valley quantum number), the valence band arises from hybridization of $d_{x^2-y^2} + \tau i d_{xy}$ orbitals with angular momentum $l_z = 2\tau\hbar$ while the conduction band arises from hybridization of d_{z^2} orbitals with $l_z = 0$ [1, 6, 23, 28]. In the tight-binding limit, we therefore expect a contribution to the exciton Zeeman energy of $2\left(E_{Z,a}^c - E_{Z,a}^v\right) = -4\mu_B B$ from atomic-scale magnetic moments. The phase winding of Bloch states on the intercellular scale can also add to the orbital magnetic moment [11, 24, 26, 27, 29]. For example, in the two-band tight-binding model (the massive Dirac fermion model) the intercellular magnetic moment is equal for the conduction and valence bands with value $-\tau\mu_B \frac{m_e}{m_{\text{eff}}}$, where m_e is the free-electron mass, and m_{eff} is the electron-hole symmetric carrier effective mass [11, 12]. Including the spin magnetic moments this gives a total Zeeman splitting of $2E_Z^c = 2\mu_B + 2\mu_B \frac{m_e}{m_{\text{eff}}}$ for the conduction band and $2E_Z^v = 2\mu_B B + 4\mu_B B + 2\mu_B B \frac{m_e}{m_{\text{eff}}}$ for the valence band, and as a result $2\left(E_Z^c - E_Z^v\right) = -4\mu_B B$ (i.e. there is no net intercellular contribution). In more general hopping models, the conduction and valence bands can have different intercellular moments giving a net contribution to the exciton magnetic moment [16, 22, 26, 27].

To compare our measurements with theory, we define the exciton valley g-factor $g_{\text{ex}}^{\text{vl}}$ as:

$$g_{\text{ex}}^{\text{vl}} = \frac{2(E_+ - E_-)}{\mu_B B} = \frac{2(E_Z^c - E_Z^v)}{\mu_B B} \tag{1}$$

where $E_\pm$ is the measured exciton peak energy in $\sigma_\pm$ detection. Our exciton valley splitting

measurements correspond to $g_{\mathrm{ex}}^{\mathrm{vl}} = -3.8 \pm 0.2$, consistent with the value of $g_{\mathrm{ex}}^{\mathrm{vl}} = -4$ expected from the d-orbital contribution to the exciton magnetic moment. Any deviation of $g_{\mathrm{ex}}^{\mathrm{vl}}$ from -4 theoretically corresponds to the intercellular contribution to the g-factor. Our results therefore suggest that the intercellular contribution to $g_{\mathrm{ex}}^{\mathrm{vl}}$ is small in the case of $MoSe_2$. We also expect the trion to have approximately the same splitting as the exciton, evinced by considering the trion as an exciton bound to an additional electron. While the additional electron contributes to the trion magnetic moment, it contributes equally to the final state moment after recombination leaving the transition energy unaffected (as discussed in more detail in supplement section 4 [21]). This is consistent with the experimental results of Fig. 3a for zero applied gate voltage.

We also attempted to calculate the valley g-factor using the multiband $\mathbf{k} \cdot \mathbf{p}$ theory of Refs. [13, 25], since their theory should include the intercellular and atomic contributions in a unified way [29]. The need to discuss these terms separately is an artifact of the lattice models discussed above. The calculation is detailed in section 5 of the supplement and gives a value for $g_{\mathrm{ex}}^{\mathrm{vl}}$ similar in magnitude to our experimental results, but with the opposite sign (see supplement section 6 for our experimental determination of the sign [21]). Therefore further theoretical work is required to understand the exciton valley splitting within the context of $\mathbf{k} \cdot \mathbf{p}$ theory calculations.

We find that the trion valley splitting and the resulting luminescence polarization both show a surprising dependence on an applied back-gate voltage. Polarization-resolved spectra taken with -20 V and 51 V applied to the substrate are shown in Fig. 4a for device D2. Our samples show significant hysteresis assumed to arise from photoionization of trap states [30], and the data in this panel are taken from a downward sweep. Figure 4b shows the trion splitting versus magnetic field for two different gate voltages on a downward sweep, finding $-0.29 \pm 0.02 \frac{\mathrm{meV}}{\mathrm{T}}$ at 40 V and $-0.23 \pm 0.02 \frac{\mathrm{meV}}{\mathrm{T}}$ at 0 V. This gate-voltage dependence of the trion splitting could arise from carrier-density dependence of the band Zeeman energies [11, 16], a hot luminescence effect as discussed in section 4 of the supplement [21], or other effects resulting from changes in the trion or final state wavefunctions upon increasing the Fermi level [31]. The gate dependence of trion valley splitting has implications for future magneto-optical studies of TMDs, as the intrinsic doping level may vary between samples causing a dispersion of measurement results.

The degree of trion polarization as a function of gate voltage is shown in Fig. 4c. In this
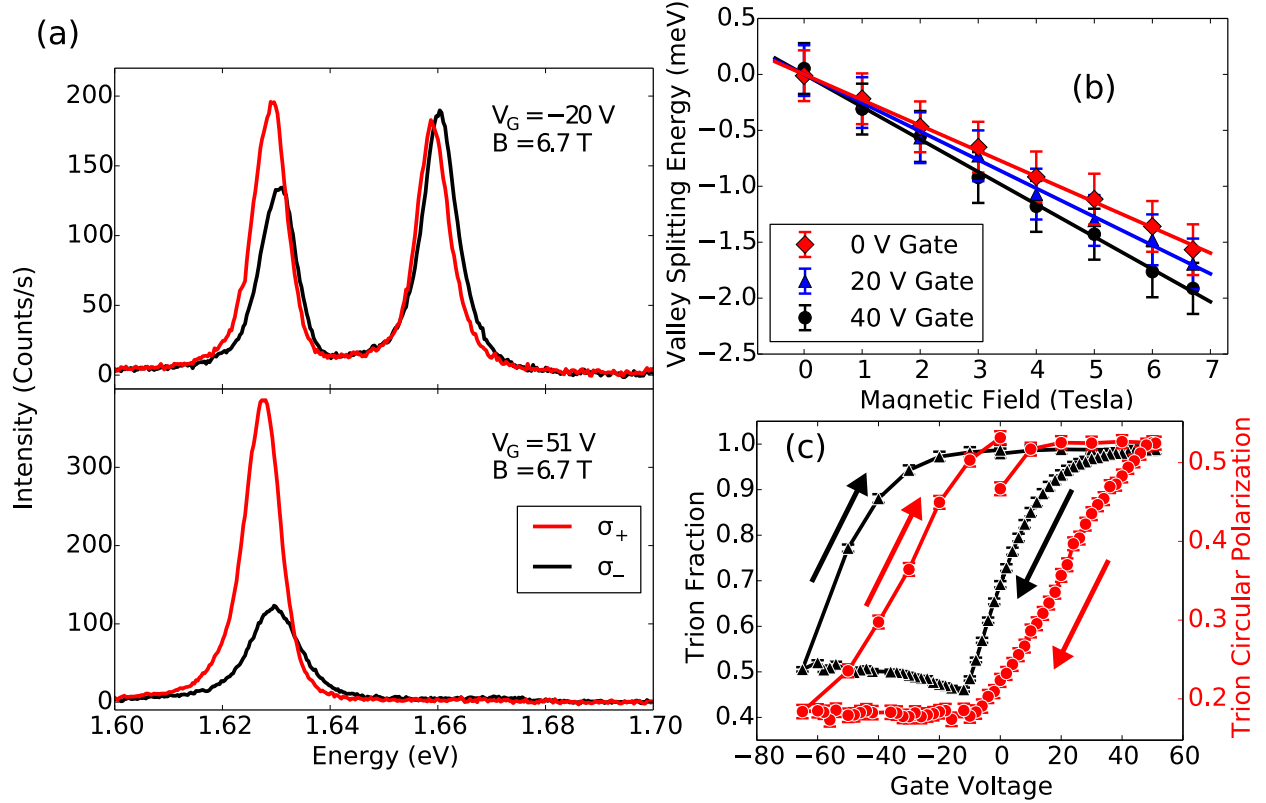
FIG. 4. (color online). (a) Polarization-resolved luminescence spectra from D2 at 4.2K and 6.7 T for σ_+ and σ_- detection, excited with σ_- light at 1.89 eV. From top to bottom the panels show spectra taken with -20 V and 51 V gate voltage applied to the substrate. (b) Trion valley splitting versus magnetic field for selected gate voltages, showing an decrease in slope with gate voltage. (c) Circular polarization of the trion peak $\frac{I_+ - I_-}{I_+ + I_-}$ versus gate voltage at 6.7 T (red circles), showing an increase to over 50% as gate voltage is increased. For comparison, we also plot the trion fraction $\frac{I_{\text{trion}}}{I_{\text{trion}} + I_{\text{exciton}}}$ (black triangles).

dataset, we find a trion polarization that increases from 18% near zero back-gate voltage to over 50% near 40 V. The luminescence polarization in the n-type regime is related to the populations of different trion species via $P_{\text{trion}} = \frac{n_+ - n_-}{n_+ + n_-}$, where $n_\pm$ is the density of negatively-charged trions with their hole in valley $K_\pm$ (i. e. those which emit $\sigma_\pm$ polarized light upon recombination, which we refer to as $K_\pm$ valley trions). The sign of P_{trion} is found to be independent of the excitation polarization and instead follows the sign of the magnetic field, and we therefore interpret the magnetic field dependence of the trion polarization as arising from partial relaxation of trions into their lowest energy spin-valley configuration

9

(qualitatively consistent with the dependence of trion polarization on excitation power, see supplement section 7 [21]). This relaxation is expected to be incomplete as the intervalley scattering time is longer than the recombination time [2]. In section 4 of the supplement, we calculate the trion polarization within a simple rate-equation model and show that the observed P_{trion} implies a ratio of the recombination time to the intervalley scattering time of ~ 0.2 at low carrier density [21]. This is about an order of magnitude larger than the value found in time-resolved measurements for WSe$_2$ at zero magnetic field [32]; however, the time-resolved measurements used resonant excitation which is expected to lead to reduced intervalley scattering compared to the off-resonant excitation we use. Trions can scatter between valleys via spin-flip intervalley scattering of their hole, and if this is the dominant scattering mechanism our results imply that the hole intervalley scattering rate increases monotonically with carrier density. This is consistent with the Bir-Aronov-Pikus mechanism for intervalley scattering of holes via their exchange interaction with the conduction electrons [2, 33]. The data in Fig. 4c were taken with σ_- excitation, but similar results were found using unpolarized excitation (see section 3 of the supplement [21]).

In summary, we have presented measurements of polarization-resolved luminescence spectra for MoSe$_2$ at 4.2 K in magnetic fields up to 6.7 T, demonstrating valley degeneracy breaking. We measure a splitting of $-0.22 \pm 0.01 \, \frac{\text{meV}}{\text{T}}$ between exciton peaks in σ_+ and σ_- polarized emission spectra. This value is consistent with a simple tight-binding picture of the MoSe$_2$ bandstructure. We also observe gate dependence of the trion valley splitting and polarization. Even with off-resonant, unpolarized excitation we were able to achieve a trion circular polarization of about 50% by gating the sample in 6.7 T magnetic field. Application of magnetic and electric fields can therefore provide an effective strategy for manipulating the valley degree of freedom in monolayer TMDs.

Similar work on WSe$_2$ has recently been posted by the Washington group [27] and the ETH Zurich group [26].

———————

[1] D. Xiao, G.-B. Liu, W. Feng, X. Xu, and W. Yao, Phys. Rev. Lett. **108**, 196802 (2012).

[2] K. F. Mak, K. He, J. Shan, and T. F. Heinz, Nat. Nanotech. **7**, 494 (2012).

[3] A. M. Jones, H. Yu, N. J. Ghimire, S. Wu, G. Aivazian, J. S. Ross, B. Zhao, J. Yan, D. G. Mandrus, D. Xiao, W. Yao, and X. Xu, Nat. Nanotech. **8**, 634 (2013).

[4] G. Kioseoglou, A. Hanbicki, M. Currie, A. Friedman, D. Gunlycke, and B. Jonker, App. Phys. Lett. **101**, 221907 (2012).

[5] H. Zeng, J. Dai, W. Yao, D. Xiao, and X. Cui, Nat. Nanotech. **7**, 490 (2012).

[6] T. Cao, G. Wang, W. Han, H. Ye, C. Zhu, J. Shi, Q. Niu, P. Tan, E. Wang, B. Liu, and J. Feng, Nat. Comm. **3**, 887 (2012).

[7] G. Sallen, L. Bouet, X. Marie, G. Wang, C. R. Zhu, W. P. Han, Y. Lu, P. H. Tan, T. Amand, B. L. Liu, and B. Urbaszek, Phys. Rev. B **86**, 081301 (2012).

[8] K. F. Mak, K. L. McGill, J. Park, and P. L. McEuen, Science **344**, 1489 (2014).

[9] J. S. Ross, S. Wu, H. Yu, N. J. Ghimire, A. M. Jones, G. Aivazian, J. Yan, D. G. Mandrus, D. Xiao, W. Yao, and X. Xu, Nat. Comm. **4**, 1474 (2013).

[10] Y. Zhang, T.-R. Chang, B. Zhou, Y.-T. Cui, H. Yan, Z. Liu, F. Schmitt, J. Lee, R. Moore, Y. Chen, H. Lin, H.-T. Jeng, S.-K. Mo, Z. Hussain, A. Bansil, and Z.-X. Shen, Nat. Nanotech. **9**, 111 (2013).

[11] D. Xiao, W. Yao, and Q. Niu, Phys. Rev. Lett. **99**, 236809 (2007).

[12] W. Yao, D. Xiao, and Q. Niu, Phys. Rev. B **77**, 235406 (2008).

[13] A. Kormányos, V. Zólyomi, N. D. Drummond, and G. Burkard, Phys. Rev. X **4**, 011034 (2014).

[14] X. Li, F. Zhang, and Q. Niu, Phys. Rev. Lett. **110**, 066803 (2013).

[15] R.-L. Chu, X. Li, S. Wu, Q. Niu, W. Yao, X. Xu, and C. Zhang, Phys. Rev. B **90**, 045427 (2014).

[16] H. Rostami, A. G. Moghaddam, and R. Asgari, Phys. Rev. B **88**, 085440 (2013).

[17] Y.-H. Ho, Y.-H. Wang, and H.-Y. Chen, Phys. Rev. B **89**, 155316 (2014).

[18] T. Cai, S. A. Yang, X. Li, F. Zhang, J. Shi, W. Yao, and Q. Niu, Phys. Rev. B **88**, 115140 (2013).

[19] A. Högele, S. Seidl, M. Kroner, K. Karrai, C. Schulhauser, O. Sqalli, J. Scrimgeour, and R. J. Warburton, Rev. Sci. Instrum. **79**, 023709 (2008).

[20] M. Sladkov, M. Bakker, A. Chaubal, D. Reuter, A. Wieck, and C. van der Wal, Rev. Sci. Instrum. **82**, 043105 (2011).

[21] See supplemental material at [url], which includes Refs. [34–51].

[22] G.-B. Liu, W.-Y. Shan, Y. Yao, W. Yao, and D. Xiao, Phys. Rev. B **88**, 085433 (2013).

[23] K. Kośmider, J. W. González, and J. Fernández-Rossier, Phys. Rev. B **88**, 245436 (2013).

[24] M.-C. Chang and Q. Niu, J. Phys.: Condens. Matter **20**, 193202 (2008).

[25] A. Kormányos, V. Zólyomi, N. D. Drummond, P. Rakyta, G. Burkard, and V. Fal'ko, Phys. Rev. B **88**, 045416 (2013).

[26] A. Srivastava, M. Sidler, A. V. Allain, D. S. Lembke, A. Kis, and A. Imamoglu, arXiv preprint arXiv:1407.2624 (2014).

[27] G. Aivazian, Z. Gong, A. M. Jones, R.-L. Chu, J. Yan, D. G. Mandrus, C. Zhang, D. Cobden, W. Yao, and X. Xu, arXiv preprint arXiv:1407.2645 (2014).

[28] Z. Y. Zhu, Y. C. Cheng, and U. Schwingenschlögl, Phys. Rev. B **84**, 153402 (2011).

[29] Y. Yafet, in *Solid State Physics Volume 14*, edited by F. Seitz and D. Turnbull (1963).

[30] A. A. Mitioglu, P. Plochocka, J. N. Jadczak, W. Escoffier, G. L. J. A. Rikken, L. Kulyuk, and D. K. Maude, Phys. Rev. B **88**, 245403 (2013).

[31] C. Zhang, H. Wang, W. Chan, C. Manolatou, and F. Rana, Phys. Rev. B **89**, 205436 (2014).

[32] G. Wang, L. Bouet, D. Lagarde, M. Vidal, A. Balocchi, T. Amand, X. Marie, and B. Urbaszek, Phys. Rev. B **90**, 075413 (2014).

[33] G. Bir, A. Aronov, and G. Pikus, Zh. Eksp. Teor. Fiz. **69**, 1382 (1975).

[34] J. Ma and Y.-S. Li, Applied Optics **35**, 2527 (1996).

[35] H. Yu, G.-B. Liu, P. Gong, X. Xu, and W. Yao, Nat. Comm. **5**, 3876 (2014).

[36] C. R. L. P. N. Jeukens, P. C. M. Christianen, J. C. Maan, D. R. Yakovlev, W. Ossau, V. P. Kochereshko, T. Wojtowicz, G. Karczewski, and J. Kossut, Phys. Rev. B **66**, 235318 (2002).

[37] J. M. Luttinger, Phys. Rev. **102**, 1030 (1956).

[38] L. M. Roth, Phys. Rev. **118**, 1534 (1960).

[39] S. Wu, J. S. Ross, G.-B. Liu, G. Aivazian, A. Jones, Z. Fei, W. Zhu, D. Xiao, W. Yao,

D. Cobden, and X. Xu, Nat. Physics **9**, 149 (2013).

[40] A. Kormányos, V. Zólyomi, M. Gmitra, N. D. Drummond, J. Fabian, V. Fal'ko, and G. Burkard, arXiv preprint arXiv:1410.6666 (2014).

[41] A. Ramasubramaniam, Phys. Rev. B **86**, 115409 (2012).

[42] R. S. Knox, *Theory of Excitons* (Academic Press New York, 1963).

[43] N. Gippius, A. Yablonskii, A. Dzyubenko, S. Tikhodeev, L. Kulik, V. Kulakovskii, and A. Forchel, J. Appl. Phys. **83**, 5410 (1998).

[44] G. Berghäuser and E. Malic, Phys. Rev. B **89**, 125309 (2014).

[45] T. C. Berkelbach, M. S. Hybertsen, and D. R. Reichman, Phys. Rev. B **88**, 045318 (2013).

[46] M. Sugawara, N. Okazaki, T. Fujii, and S. Yamazaki, Phys. Rev. B **48**, 8848 (1993).

[47] H. Q. Hou, W. Staguhn, S. Takeyama, N. Miura, Y. Segawa, Y. Aoyagi, and S. Namba, Phys. Rev. B **43**, 4152 (1991).

[48] D. C. Rogers, J. Singleton, R. J. Nicholas, C. T. Foxon, and K. Woodbridge, Phys. Rev. B **34**, 4002 (1986).

[49] A. Malyavkin, Solid State Commun. **39**, 1315 (1981).

[50] E. Molva and L. S. Dang, Phys. Rev. B **27**, 6222 (1983).

[51] E. Molva and L. S. Dang, Phys. Rev. B **32**, 1156 (1985).